Malaysian Journal of Analytical Sciences, Vol 20 No 4 (2016): 892 - 900
DOI: http://dx.doi.org/10.17576/mjas-2016-2004-25

MALAYSIAN JOURNAL OF ANALYTICAL SCIENCES
Published by The Malaysian Analytical Sciences Society
ISSN 1394 - 2506

TiO_2 DOPED WITH Fe_2O_3 FOR PHOTOELECTROCHEMICAL WATER SPLITTING ELECTRODE: EXPERIMENTAL AND DENSITY FUNCTIONAL THEORY STUDY

(TiO_2 Di Dop Bersama Fe_2O_3 untuk Elektrod Pembelahan Molekul Air Secara Fotoelektrokimia: Eksperimen dan Kajian Teori Fungsi Ketumpatan)

Khuzaimah Arifin[1*], Hasmida Abdul Kadir[1,3], Lorna Jeffery Minggu[1], Wan Ramli Wan Daud[1,2], Mohammad B. Kassim[1,3]

[1]*Fuel Cell Institute*
[2]*Department of Chemical and Process Engineering*
[3]*School of Chemical Sciences and Food Technology, Faculty of Science and Technology*
Universiti Kebangsaan Malaysia, 43600 UKM Bangi, Selangor, Malaysia

**Corresponding author: khuzaim@ukm.edu.my*

Received: 5 February 2016; Accepted: 22 April 2016

Abstract

Various modifications of the titanium dioxide thin films have been done in fulfilling the photoelectrode requirements for photoelectrochemical water splitting reaction. In this study, surface passivation of TiO_2 by hematite-Fe_2O_3 was reported. Electrodeposition technique was used to deposit the Fe_2O_3 onto the TiO_2/FTO film with variation of time. X-ray diffraction (XRD), Scanning Electron Microscope (SEM) and UV-Vis spectroscopic analyses were used to characterize the electrode. Plane-wave-based pseudopotential density functional theory (DFT) calculations were used to analyze the electronic structure and charge potential at the surface of the electrode. The photocurrent measurement showed that current density of TiO_2/Fe_2O_3 electrode was higher than the TiO_2/FTO under the same illumination intensity of 100 $mWcm^{-2}$. The highest current density was produced by 5 minutes electrodeposition of Fe_2O_3, which also shifted the absorption to visible region at the threshold wavelength of 518 nm.

Keywords : titanium dioxide, iron(III) oxide, passivation layer, band gap

Abstrak

Pelbagai pengubahsuaian titanium dioksida filem nipis telah dilakukan untuk memenuhi keperluan fotoelektrod bagi tindak balas fotoelektrokimia pembelahan molekul air. Dalam kajian ini, dilaporkan pempasifan permukaan TiO_2 dengan bijih besi-Fe_2O_3. Teknik pengelektroenapan digunakan untuk mendepositkan Fe_2O_3 ke TiO_2/FTO filem dengan pelbagai masa pengelektroenapan. Analisis XRD, SEM dan UV-Vis spektroskopi telah digunakan untuk mencirikan elektrod. pengiraan teori fungsi ketumpatan (DFT) berasaskan planar gelombang pseudopotential telah digunakan untuk menganalisis struktur elektronik dan potensi caj di permukaan elektrod. Pengukuran arusfoto menunjukkan bahawa ketumpatan arus TiO_2/Fe_2O_3 elektrod adalah lebih tinggi daripada TiO_2/FTO bawah keamatan pencahayaan yang sama, 100 $mWcm^{-2}$. Ketumpatan semasa tertinggi dihasilkan oleh 5 minit pengelektroenapan Fe_2O_3, yang mana penyerapan beralih ke kawasan yang boleh dilihat pada panjang gelombang ambang 518 nm.

Kata kunci: titanium dioksida, ferum (III) oksida, lapisan pasif, sela jalur

Introduction

Hydrogen has been considered as an alternative fuel to replace fossil fuels for many years. It is used in fuel cell technology to generate electricity where water molecule is the only byproduct [1]. Hydrogen is plentiful in the universe, obtained via extraction off water molecule, an element, which is abundant and cheap; however requires a lot of energy to extract it. One of the promising method to produce hydrogen from water molecule is through photoelectrochemical (PEC) reaction that utilizes sunlight energy [2]. The system uses inexpensive metal oxide photoelectrode without the expense of electrolyzer, which leads to a further reduction in the cost of hydrogen delivery. The concept was first demonstrated by Honda and Fujishima in 1972 and since then, its science has influenced many followers [3].

PEC cell is a type of an electrolytic cell, where the sunlight is absorbed by the photoelectrode to generate current that is used to drive an electrochemical reaction. Generally, photoelectrode is an n or a p-type semiconductor electrode, which flows the electrons generated by the light induced chemical reactions initiated at its surface. Several photoelectrode requirements that must be fulfilled for direct PEC water splitting to occur are listed in Table 1. The band gap of photoelectrode semiconductor must be at least 1.5 eV, higher than the effective redox potential of water, which is about 1.23 – 1.4 eV [4,5].

Table 1. Main PEC water-splitting requirements [4]

Condition	**Requirement**
PEC water-splitting	$H_2O_{(liquid)} + 2h\upsilon \rightarrow ½O_{2(gas)} + H_{2(gas)}$
Minimum potential	$E°_{H_2O}(25\ °C)_{min} = 1.229$ eV
Practical potential (+overpotential & losses)	$E°_{H_2O}(25\ °C)_{prac} = 1.6 - 2.0$ eV $E_{bandgap} > E°_{H_2O}$
Utilization of sunlight	UV > hυ (Vis) > IR $h\upsilon \geq E_{bandgap}$
Bandedges	$C_{band\ edge} < E°_{H2/H^+}$ $V_{band\ edge} > E°_{O2/H2O}$

Concurrently, the semiconductor's conduction band (CB) must be higher than the reduction potential of water, whle its valence level (VB) must be lower than the oxidation potential of water. The focus of recent PEC research are mostly on developing photoelectrode materials that meet with the criteria besides high efficiencies, low-cost, long-term usages and non-photocorrosion of materials [3].

Titanium dioxide (TiO_2) is reported as the most promising photoelectrode [6]. This material has several advantages for photochemistry and photo-electrochemistry including low cost, widely available, non-photocorrosion and nontoxic. However, TiO_2 photocatalytic has large band gaps that limit its absorption of solar radiation to just 4 %, which is of UV spectrum. Numerous attempts have been made to expand the TiO_2 photoanode absorption spectrum to longer wavelengths: through doping TiO_2 with various metals and anions, use a dye-sensitizer molecule [7] and also morphology modifications of nano-scaled TiO_2, namely spheres, wires, rods and tubes [8, 9]. Significant experimental results are also observed by a surface passivation layer of TiO_2 with various metal oxide [10, 11]. Surface passivation layers electrode is a type of junction electrode, which comprises two or more layers of semiconductors. The surface passivation layers provide an alternative low energy route for charge transfer through catalytically active sites. In addition, surface passivation layers can reduce corrosion and improve chemical or photochemical stability of photoelectrode when immersed in an electrolyte [3,12].

In designing the passivation layer, it is important to consider the band positions of the metal oxides (Figure 1). For wide band gap semiconductor, TiO_2 should be combined with a narrow band gap metal oxide: WO_3 [13], Cu_2O

[14], CdTe [15] and CdS [16], that can absorb visible light. Here, investigation TiO_2 passivated by hematite-Fe_2O_3 is reported. Fe_2O_3 is one of prospective material for PEC. It is a photoactive material and absorbs visible light, however is poor in conductivity and has a CB energy below the reduction potential of hydrogen ion [11].

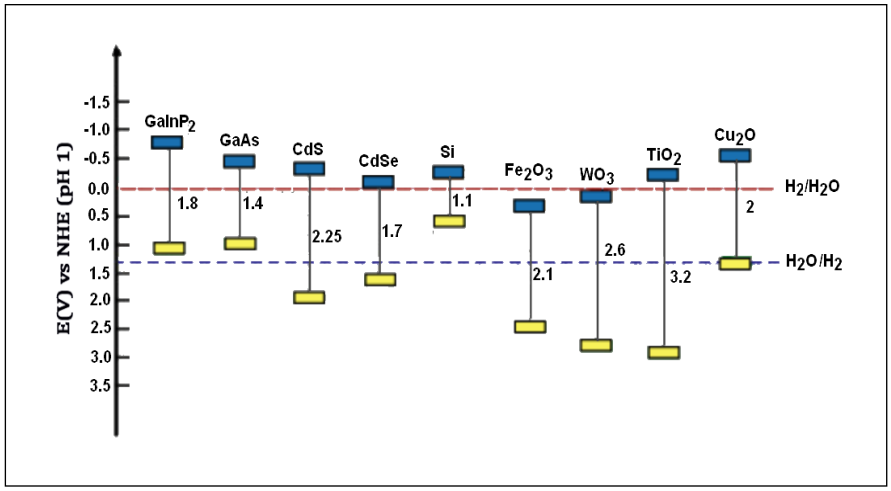

Figure 1. Bandgap and band edges of some semiconductor materials compared with a redox potential of water molecules

In this study, the Fe_2O_3 was electrodeposited on the TiO_2/ FTO thin film by variation of time. The Fe_2O_3/TiO_2/FTO multilayer film system was characterized by X-ray diffraction (XRD), Scanning Electron Microscope (SEM) and Uv-vis spectroscopy. PEC performance was measured by calculating its I-V under UV–vis light illumination.

Materials and Methods

Photoelectrode preparation

The TiO_2 electrodes were prepared using commercial colloidal TiO_2 powder (Degussa P25) by doctor-blading onto fluorine-doped tin oxide (FTO) glass plates. The 1 g TiO_2 powder was ground with 1 ml dipolyethylene glycol 300 (Merck), Triton-X and double-distilled water to form homogenous paste. The paste was smeared onto a clean FTO glass. Then, the TiO_2/FTO was dried at room temperature for a few minutes and was heated in a furnace at 450 ^oC for 2 hours with ramping rate of 5 $^oC\ s^{-1}$. Afterward, the Fe_2O_3 was deposited onto the TiO_2/FTO using electrodeposition method for 5 minutes, in which the iron sulfate ($FeSO_4$) was used as the starting material. The process was carried out using a potentiostat (VersaSTAT 4, Ametek), connected to a working electrode (TiO_2/FTO), counter electrode (Pt) and reference electrode (Saturated Calomel Electrode, SCE). The samples were calcined in a furnace at 500 ^oC for 60 minutes with heating rate of 1 $^oC\ s^{-1}$. Characterization of thin films was done using X-Ray diffraction (Bruker D8 Advance) via Cu Kα radiation. Morphology of the thin film was characterized using scanning electron microscopy (Zeiss AM10).

Photoelectrochemical analysis

The PEC analysis was conducted based on previous study [17]. The analyses were carried out using Ametek Versastat 4 on the TiO_2 and TiO_2 deposited by Fe_2O_3 at different times. The 450 W full arc Xenon light source at an intensity of 100 $mWcm^{-2}$ was used to irradiate the electrodes. The electrolyte in this experiment was 0.5 M Na_2SO_4, and it was purged with nitrogen gas for 30 min before the tests. The scan rate was set to 0.01 $V\ s^{-1}$.

Computational method

Density functional theory (DFT) calculations were carried out using the $DMol^3$ code in Materials Studio 5.5 from Accelrys. Geometry of the bulk molecule was optimized in a double-numeric-plus polarization (DNP) basis, set

using three different functional methods: PWC, PW91 and PBE. Self-consistent field (SCF) method was used for calculating the electronic structure; all core electrons were treated as being polarizable and Hartree-Folk (RHF) spin-restricted mode. TDDFT calculations were conducted on the ground state in spin-restricted mode.

Results and Discussion

X-ray diffraction (XRD) patterns of the TiO_2 and TiO_2/Fe_2O_3 on the FTO films are shown in Figure 2. The TiO_2 anatase (101) phase was observed at 25.35°, while rutile (110) phase appered at 27.40° (Figure 2b). The peaks for α-Fe_2O_3 (104) appeared at 33.50°, while α-Fe_2O_3(110) at 35.50° (Figure 2c) (JCPDS file no. 01-077-9926). All TiO_2 and Fe_2O_3 peaks were observed at TiO_2/Fe_2O_3 composite pattern (Figure 2d). Diffractogram pattern of the TiO_2 produced is similar with TiO_2 pattern that was reported by Vlasa et al. [18].

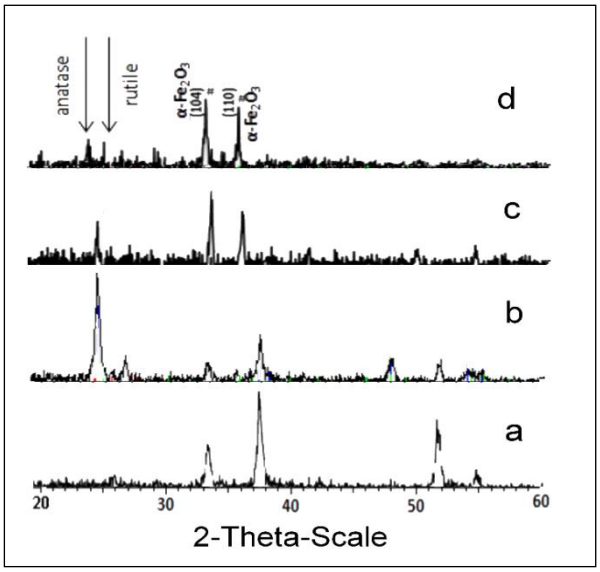

Figure 2. X-ray diffraction for (a) FTO (b) TiO_2 and (c) Fe_2O_3 and (d) TiO_2/Fe_2O_3

The surface morphology by scanning electron microscopic (SEM) image of TiO_2/Fe_2O_3 on an FTO glass substrate is shown in Figure 3. The image clearly shows flower-like shape on the surface of TiO_2 substrate (B), which is similar to a previous study [19]. The duration of deposition time changed the shape of Fe_2O_3; at 3 minutes, the flower-like shape changed to a spiny and globular structure (C) and then turned to fine particles that scattered randomly onto TiO_2 surface at 5 minutes (D). The presence of Fe was confirmed by EDX analysis (Table 2). The number of Fe did not automatically increased with time of deposition; however, the shape of Fe was: at 5 minutes of deposition time, the Fe shape became clotted and the TiO_2 surface became exposed. The thickness of TiO_2/Fe_2O_3 layer on the FTO substrate based on SEM images was obtained around 10-15 μm.

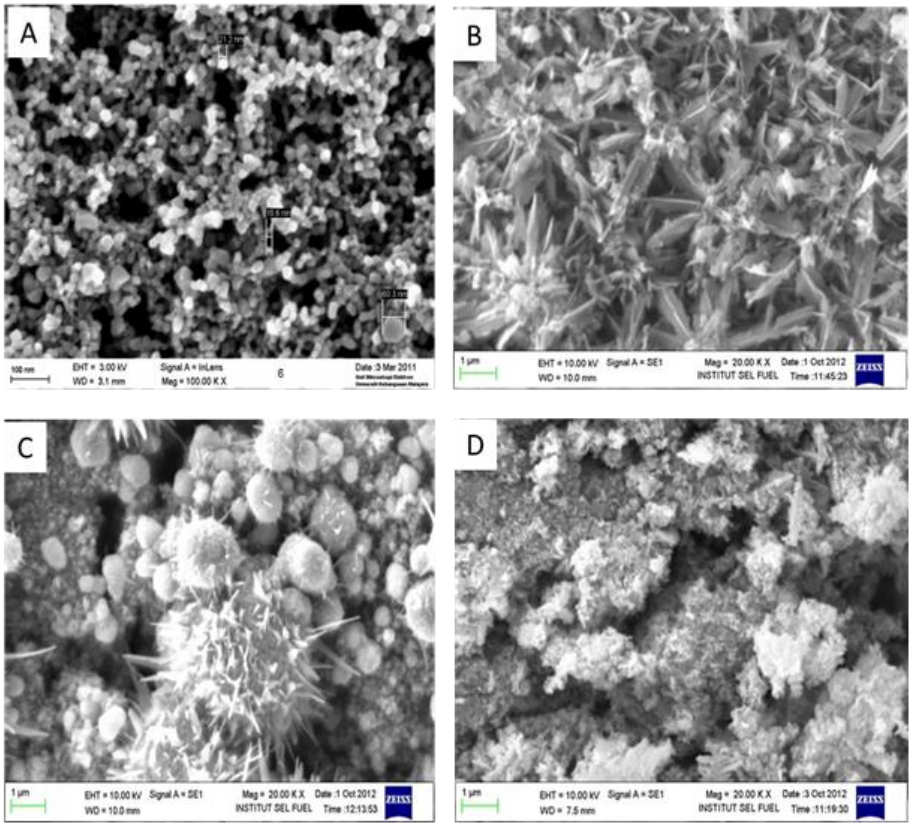

Figure 3. Surface morphology of (a) TiO_2 and (b) TiO_2/Fe_2O_3 on FTO films

Table 2. Element percentage of Fe, Ti and O based on EDX analysis

Element	Percentage (%) of element		
	TiO_2-Fe_2O_3 (1 min)	**TiO_2-Fe_2O_3 (3 min)**	**TiO_2-Fe_2O_3 (5 min)**
Ferrum (Fe)	57.0	29.8	16.3
Titanium (Ti)	55.6	42.8	18.6
Oxygen (O)	28.2	27.4	24.4

The optical characterizations of TiO_2 and TiO_2 doped Fe_2O_3 are shown in Figure 4. The band gaps were determined from reflectance spectra of the films using the following formula equation 1[5]:

$$E_g\ (eV) = 1240/\lambda_g\ (nm) \quad (1)$$

where, E_g and λ_g are the band gap energy and the absorption wavelength threshold of the doping material, respectively. In Figure 4, the band gap of TiO_2 was found to be 3.44 eV with the threshold wavelength at 360 nm. On the other hand, band gap of the TiO_2 doped with Fe_2O_3 was 2.39 eV with the threshold wavelength at 518 nm. The TiO_2/Fe_2O_3 film absorption was shifted to visible light, caused by excitation of electrons in the 3d shell of Fe to conduction band of TiO_2 [20].

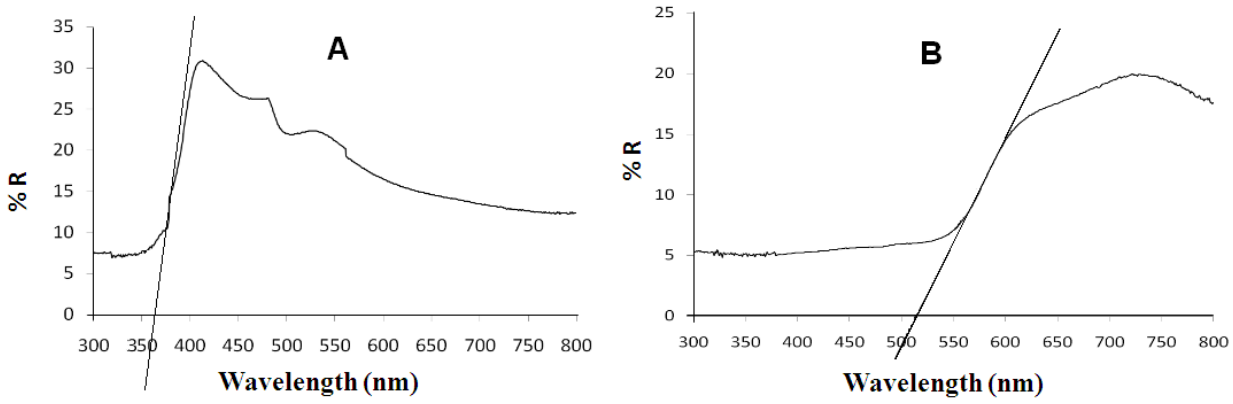

Figure 4. Reflection (R) spectra of TiO_2 (**A**) and TiO_2 doped Fe_2O_3 (5 min) (**B**) electrodes

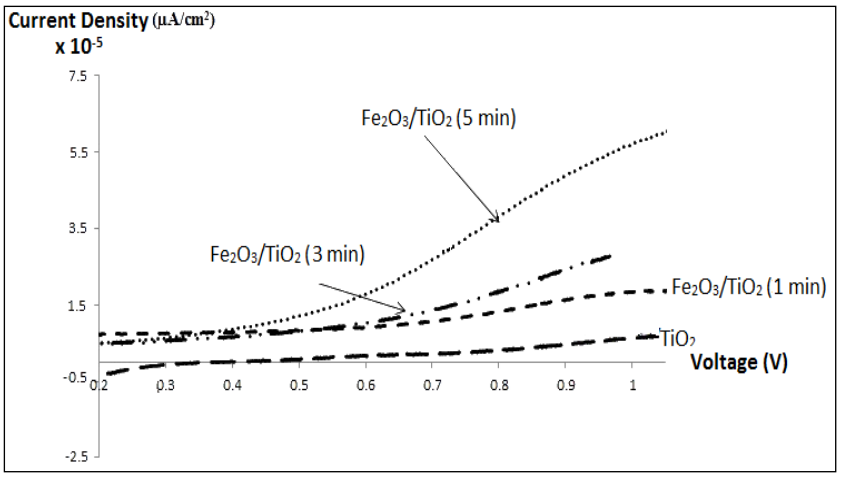

Figure 5. Current density-voltage (V/SCE) characteristics for Fe_2O_3/TiO_2 at different duration of electrodeposition proses

Photocurrent density was measured using three electrodes in 0.5 M Na_2SO_4 electrolyte under a Xenon lamp (100 mW cm^{-2}) irradiation. The applied voltage bias was measured againts SCE as the reference, and the values of photocurrent are shown in Figure 5. The current density of undoped TiO_2 was low compared with TiO_2 doped with Fe_2O_3. In addition, the deposition time of Fe_2O_3 onto TiO_2 surface contributed to the increase of current density. The highest photocurrent was measured at 5 minutes deposition of Fe_2O_3, which was about 55 µA cm^{-2} at 1.0 V bias potential. The current density of TiO_2 without Fe_2O_3 is 7 µAcm^{-2} and TiO_2/Fe_2O_3 at 1 and 3 minutes are 28 µAcm^{-2} and 29 µAcm^{-2}, respectively. This is probably due to the reduction of electron-hole recombination on TiO_2 doped with Fe_2O_3. Kim et al. found similar result, where the passivation layer of TiO_2 with Fe_2O_3 as photo-absorber on FTO film showed 3.5 times higher photocurrent densities for water splitting under UV-vis light illumination than the Fe_2O_3/FTO or TiO_2/FTO films [11].

Theoretical investigation started with the optimization of the bulk structure of TiO_2 and Fe_2O_3 in three kinds of functional methods. The average length of Ti-O and Fe-O are shown in Table 3. Calculated bond length of the Ti-O in these three methods gave similar results, which was about 1.92 Å. The calculated bond length of the Fe-O in

PWC was about 0.03 Å smaller than the calculated PW91 and PBE, which was about 1.96 Å. All calculated bond lengths of the Ti-O and Fe-O were in normal range [16]. The band gap of TiO_2 and Fe_2O_3 in these three methods were similar at about 0.076 Ha (2.06 eV) and 0.03 Ha (0.81 eV), respectively (Figure 6). Although the calculated band gaps were smaller than the experimental data, it is aceptable since the calculations were in atomic level.

Table 3. Bond length (Å) of the optimized structure in three different functional method calculation.

Bulk	**LDA-PWC**	**GGA-PW91**	**GGA-PBE**
Ti-O	1,923	1,927	1,927
Fe-O	1,939	1,960	1,960

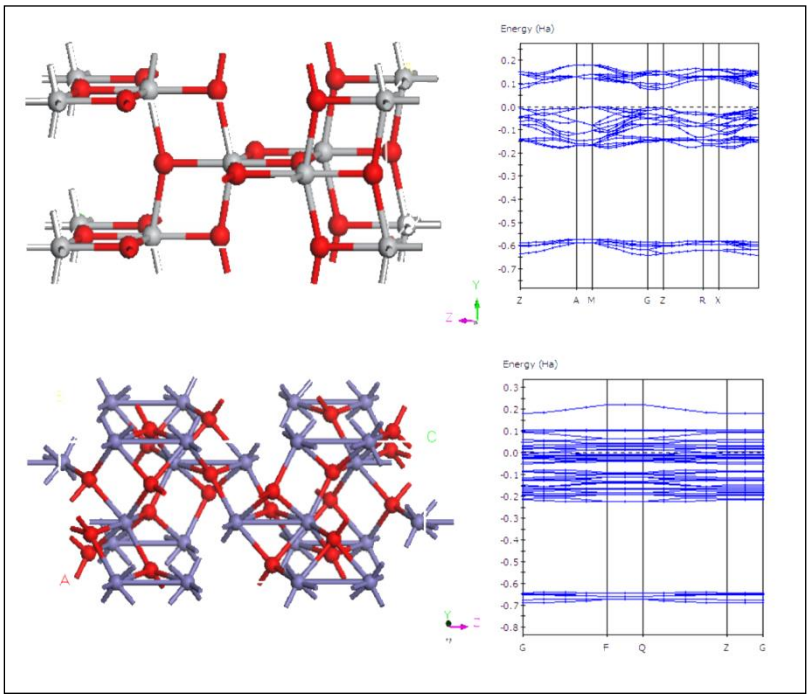

Figure 6. Molecular structure and electronic structure of TiO_2 (101), Fe_2O_3 (104) and composite TiO_2/Fe_2O_3

The optimized bulk structures of TiO_2 and Fe_2O_3 were used to form TiO_2 (101) and Fe_2O_3 (104) phases, which were then re-optimized further. The molecular structure of TiO_2 (101)/Fe_2O_3 (104) bilayer is shown in Figure 7. The electronic structure of the bilayer can not be determined easily since the increasing atomic number causes overlapping of the electronic orbitals. Nevertheless, band gap of the composite can be determined from the calculation of HOMO-LUMO energy gaps (0.70 eV), which is smaller than the monolayer oxides bad gaps; an indication of the charge transfer improvement in the system. Also shown in Figure 7 the potential electrophilic charge of the composite surface, where the potential of both oxides are similar. The more positive charge was found around Fe atoms, where supposedly the location of oxygen atom oxidation.

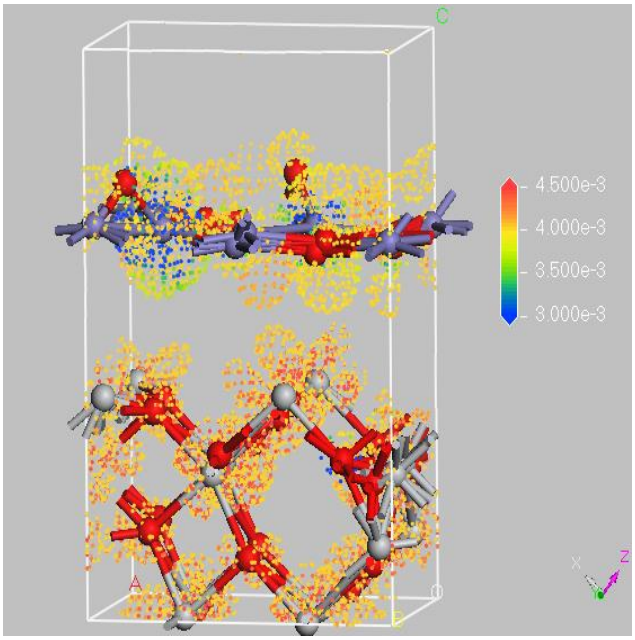

Figure 7. Molecular structure and electrophilic charge of TiO_2 (101)/Fe_2O_3 (104) composite

Conclusion

Surface passivation layer of TiO_2/Fe_2O_3 for use in the PEC water splitting application was successfully fabricated. $FeSO_4$ was used as the starting material and electrodeposition technique was used to deposit the iron molecule onto TiO_2 thin film. The measurements from photocurrent and reflection spectrum showed that Fe_2O_3 increased the performance of TiO_2 electrode. The maximum photocurrent was obtained from 5 minutes electrodeposition of Fe_2O_3 on TiO_2/FTO film. The TiO_2/Fe_2O_3 composite structure was built based on DFT calculations. The potential charges of the composite surface were successfully determined.

Acknowledgement

The authors would like to acknowledge Universiti Kebangsaan Malaysia for sponsoring this project under UKM-GUP-2011-369 and UKM-AP-TK-05-2009 research grants.

References

1. Arifin, K., Majlan, E.H., Daud, W. R.W. and Kassim, M.B. (2012). Bimetallic complexes in artificial photosynthesis for hydrogen production: A review. *International Journal of Hydrogen Energy*, 37: 3066 – 3087.
2. Currao, A. (2007) Photoelectrochemical water splitting. *Chimia*, 61: 815 – 819.
3. Liu, R., Zheng, Z., Spurgeon, J. and Yang, X. (2014). Enhanced photoelectrochemical water-splitting performance of semiconductors by surface passivation layers. *Energy and Environmental Science*, 7: 2504 – 2517.
4. Minggu, L. J., Daud, W. R.W. and Kassim, M. B. (2010). An overview of photocells and photoreactors for photoelectrochemical water splitting. *International Journal of Hydrogen Energy*, 3(35): 5233 – 5244.
5. Arifin, K., Daud, W. R.W. and Kassim, M.B. (2013). Optical and photoelectrochemical properties of a TiO_2 thin film doped with a ruthenium-tungsten bimetallic complex. *Ceramics International*, 39: 2699 – 2707.
6. Fujishima, A., Zhang, X. and Tryk, D.A. (2008). TiO_2 photocatalysis and related surface phenomena. *Surface Science Reports*, 63: 515 – 582.
7. Arifin, K., Daud, W. R.W. and Kassim, M.B. (2014). A novel ruthenium-tungsten bimetallic complex dye-sensitizer for photoelectrochemical cells application. *Sains Malaysiana*, 43(1): 95 – 101.

8. Ni, M., Leung, M. K. H., Leung, D.Y.C. and Sumathy, K. (2007). A review and recent developments in photocatalytic water-splitting using TiO_2 for hydrogen production. *Renewable and Sustainable Energy Review,* 11: 401 – 425.
9. Lin, F. and Boettcher, S.W. (2013). Adaptive semiconductor/electrocatalyst junctions in water-splitting photoanodes. *Nature Materials*, 13: 81 – 86.
10. Cao, C., Hu, C., Shen, W., Wang, S., Tian, Y. and Wang, X. (2012). Synthesis and characterization of TiO_2/CdS core–shell nanorod arrays and their photoelectrochemical property. *Journal of Alloys and Compounds* 523: 139 – 145.
11. Kim, B-R., Oh, H-J., Yun, K-S., Jung, S-C., Kang, W. and Kim, S-J. (2013). Effect of TiO_2 supporting layer on Fe_2O_3 photoanode for efficientwater splitting. *Progress in Organic Coatings,* 76:1869 – 1873
12. Fitzmorris, R. C. and Zhang, J. Z. (2015). Recent advances in metal oxide-based photoelectrochemical hydrogen production. In: Andrews D.L., editors. Photonics, Volume 2: Nanophotonic Structures and Materials, Canada, John Willey & Son. pp 346 – 358.
13. Smith, W., Wolcott, A., Fitzmorris, R. C., Zhang, J. Z. and Zhao, Y. (2011). Quasi-core-shell TiO_2/WO_3 and WO_3/TiO_2 nanorod arrays fabricated by glancing angle deposition for solar water splitting. *Journal of Material Chemistry,* 21**:** 10792 – 10800.
14. Minggu, L. J., Ng, K. H., Kadir, H. A. and Kassim, M. B. (2014). Bilayer n-WO_3/p-Cu_2O hotoelectrode with photocurrent enhancement in aqueous electrolyte photoelectrochemical reaction. *Ceramics International,* 40: 16015 – 16021.
15. Wang, Q., Yang, X., Chi, L. and Cui, M. (2013). Photoelectrochemical performance of CdTe sensitized TiO_2 nanotube array photoelectrodes. *Electrochimica Acta,* 91: 330 – 336.
16. Zhong, M., Shi, J., Xiong, F., Zhang, W. and Li, C. (2012). Enhancement of photoelectrochemical activity of nanocrystalline CdS photoanode by surface modification with TiO_2 for hydrogen production and electricity generation. *Solar Energy,* 86: 756 – 763.
17. Hang, N. K., Minggu, L.J. and Kassim, M.B. (2013). Gallium-doped tungsten trioxide thin film photoelectrodes for photoelectrochemical water splitting. *International Journal of Hydrogen Energy*, 38: 9585 – 9591.
18. Vlasa, A., Varvara, S., Pop, A., Bulea, C. and Muresan, L.M. (2010). Electrodeposited Zn–TiO_2 nanocomposite coatings and their corrosion behavior. *Journal of Applied Electrochemistry*, 40: 1519 –1527.
19. Zanganeh, S., Torabi, M., Kajbafvala, A., Zanganeh, N., Bayati, M.R., Molaei, R., Zangar, H.R. and Sadrnezhaad, S. K. (2010). CVD fabrication of carbon nanotubes on electrodeposited flower-like Fe nanostructures. *Journal of Alloys & Compounds,* 507: 494 – 497.
20. Khan, M. A., Woo, S. I. and Yang, O-B. (2008). Hydrothermally stabilized Fe(III) doped titania active under visible light for water splitting reaction. *International Journal of Hydrogen Energy,* 33: 5345 –5351.